INSTITUTE OF PHYSICS PUBLISHING SUPERCONDUCTOR SCIENCE AND TECHNOLOGY

Supercond. Sci. Technol. **18** (2005) 1–8 doi:10.1088/0953-2048/18/1/001

# Interface transparency and proximity effect in Nb/Cu triple layers realized by sputtering and molecular beam epitaxy

**A Tesauro, A Aurigemma, C Cirillo, S L Prischepa[1], M Salvato and C Attanasio[2]**

Dipartimento di Fisica 'E R Caianiello' and INFM-Laboratorio Regionale Supermat, Università degli Studi di Salerno, Baronissi (Sa), I-84081, Italy

E-mail: attanasio@sa.infn.it

Received 9 June 2004, in final form 9 June 2004
Published 16 November 2004
Online at stacks.iop.org/SUST/18/1

**Abstract**

We have investigated, in the framework of the proximity effect theory, the interface transparency $\mathcal{T}$ between Nb and Cu in the case of high quality Nb/Cu trilayers fabricated by molecular beam epitaxy (MBE) and sputtering deposition techniques. The obtained $\mathcal{T}$ values do not seem to be strongly influenced by the fabrication methods but more by the intrinsic properties of the two metals; a slightly higher value for $\mathcal{T}$ has even been deduced for the MBE prepared samples. The proximity effect in these samples has also been studied in the presence of an external magnetic field. In the parallel configuration a significant shift towards lower values of the 2D–3D crossover temperature has been observed for MBE samples, in good agreement with very recent theoretical predictions. In the perpendicular case a positive curvature of the temperature dependence of the upper critical field has been detected, which was less pronounced for sputtered samples. Both the effects have been observed only for trilayers with low Nb thickness (<600 Å) which confirms the crucial influence of the interface transparency on the values of the upper critical field in such samples.

(Some figures in this article are in colour only in the electronic version)



## 1. Introduction

In recent years an important parameter, the interface transparency $\mathcal{T}$, has been added to the description of the proximity effect between a superconductor (S) and another material (M), and many papers have recently been devoted to the study of this physical quantity for different combinations of S and M in layered structures [1–7]. Transparency can be connected with the boundary resistance that electrons encounter at the interface and that reduces the migration of the Cooper pairs from the S to the M layer. This parameter is related to the effects which cause electrons to be reflected rather than transmitted at the interfaces and it depends on both extrinsic (interface imperfections or fabrication methods) [8] and intrinsic factors (difference between Fermi velocities, band-structure and lattice structure of the two metals) [3]. However, when M is magnetic the problem is more complicated due to the role played by the splitting of the spin sub-bands and the spin-dependent impurity scattering [9]. From a theoretical point of view the interface transparency is then related to microscopic properties of metals whereas from a practical point of view it is an essential parameter to take into account in the achievement of devices based on coupling between different materials [10–13]. Very recently the influence of the boundary resistance in layered systems has also been considered in the presence of external magnetic fields [14]. When the field is applied in the direction perpendicular to the interface, the influence of the boundary is weak because the Cooper pairs move in the plane, but some

[1] Permanent address: State University of Computer Science and RadioElectronics, P Brovka Street 6, 220600, Minsk, Belarus.
[2] Author to whom any correspondence should be addressed.

features can be present in the curvature of $H_{C2\perp}(T)$ close to the critical temperature [15]. On the other hand, when the field is applied in the parallel direction, the Cooper pairs move in such a way as to cross the boundaries and the interface transparency plays an important role. For small $\mathcal{T}$ the proximity effect is weak, giving at fixed field a high value of the superconducting critical temperature. Moreover, if present, the well known 2D–3D crossover appears at higher temperatures for small values of the interface transparency [14].

Among the different causes that influence the boundary resistance between the different layers, the deposition techniques could play an important role. Depending on the physical mechanism of the growth, the deposition rate and the pressure, the interface can be more or less rough and the roughness can be more or less correlated in the lateral and vertical directions giving rise to the formation of microscopic scattering centres. These can influence the motion of the carriers at the interfaces causing a decrease of $\mathcal{T}$ from its ideal value. The study of the interface quality in the multilayers, together with the transport properties, can then allow us to discriminate between the different factors that influence the $\mathcal{T}$ value. This can be done evaluating $\mathcal{T}$ for different sets of samples obtained by different deposition techniques and appropriately analysing their structures and interfaces.

With this purpose we have investigated the interface transparency of Nb/Cu. This is the best studied S/normal metal (N) proximity coupled multilayer [16, 17] and, even very recently, many papers have been devoted to studying fundamental physical properties of this system [14, 15, 18, 19]. The samples have been prepared by using two different deposition techniques, sputtering and molecular beam epitaxy (MBE). These techniques are based on different physical principles, erosion of a target caused by energetic particles in the case of sputtering and evaporation of the sources in the case of MBE. Moreover, the different deposition conditions (starting pressure, deposition rates, growth pressure) which are usually adopted in the two systems can influence the dynamic of growth and, in particular, the crystal structure and the interface roughness. In order to get deep insight into the interface and crystal structure quality, x-ray reflectivity and diffraction analysis have been widely used. This allowed us to point out the difference between the interfaces and the structural properties of the samples obtained with the two deposition methods in order to understand how extrinsic factors, such as roughness at the interface and grains orientation, can influence $\mathcal{T}$. Moreover, in the light of the recent theoretical results for proximity systems in external fields [14], we have measured the upper critical magnetic fields of these systems to see how their behaviour as a function of the temperature is influenced by different values of the interface transparency.

## 2. Theoretical background

Interfaces between different materials are never fully transparent. For an S/N system, mechanisms which can reduce transparency are mainly impurity scattering and mismatch of Fermi velocities. In the free electron model the interface transparency due to the Fermi velocities is given by [3]

$$\mathcal{T} = \frac{4k_N k_S}{[k_N + k_S]^2} \tag{1}$$

where $k_{N,S} = m v^F_{N,S}/\hbar$ are the projections of Fermi wavevectors of N and S metals on the direction perpendicular to the interface.

The model used to describe the dependence of the superconducting critical temperature $T_C$ on the thickness of the S layer $d_S$ for N/S/N trilayers is based on the microscopic Usadel equations [20] with the boundary conditions at the interface derived by Kupriyanov and Lukichev [1]. Against this background the theory proposed by Golubov [2] for the $T_C$ determination of a N/S/N structure is based on the solution of the system of algebraic equations

$$\Omega \tan\left(\frac{\Omega\, d_S}{2\xi_S}\right) = \frac{\gamma}{\gamma_b} \tag{2}$$

$$\Psi\left(\frac{1}{2} + \frac{\Omega^2 T_{CS}}{2T_C}\right) - \Psi\left(\frac{1}{2}\right) = \ln\left(\frac{T_{CS}}{T_C}\right), \qquad \frac{T_C}{T_{CS}} \gg \frac{\gamma}{\gamma_b} \tag{3}$$

with the identification of the Abrikosov–Gorkov pair breaking parameter $\rho = \pi T_C \Omega^2 = \pi T_C(\gamma/\gamma_b)(2\xi_S/d_S)$ where $\Psi(x)$ is the digamma function, $T_{CS}$ is the bulk critical temperature of the S layer and $\xi_S$ is the superconducting coherence length. The theory of Golubov depends on two parameters, $\gamma$ and $\gamma_b$, defined as

$$\gamma = \frac{\rho_S \xi_S}{\rho_N \xi_N}, \qquad \gamma_b = \frac{R_B}{\rho_N \xi_N} \tag{4}$$

where $\rho_S$ and $\rho_N$ are the low temperature resistivities of S and N, respectively, while $R_B$ is the normal state boundary resistivity times its area. Here $\xi_N$ is the normal metal coherence length. $\gamma_b$ is related to the transparency $\mathcal{T}$ by the relation

$$\mathcal{T} = \frac{1}{1 + \gamma_b}. \tag{5}$$

The parameter $\gamma$ can be determined, by measuring $\rho_S$ and $\rho_N$ and by estimating $\xi_S$ and $\xi_N$. In this way, $\mathcal{T}$ remains the only free parameter, which can be extracted by a fitting procedure of the $T_C$ versus $d_S$ data.

## 3. Sample preparation

High quality samples were grown by MBE and by a dual-source magnetically enhanced dc triode sputtering system on Si(100) substrates kept at room temperature. Cu/Nb/Cu trilayers, with external layers of normal metal with constant thickness and an internal layer of superconducting material with variable thickness, were used to determine the dependence of $T_C$ on $d_S$. Nb/Cu/Nb trilayers, with external layers of superconducting metal with constant thickness and an internal layer of normal material with variable thickness, $d_N$, were instead used to estimate the normal coherence length by the variation of $T_C$ with $d_N$.

The two deposition techniques we have used are characterized by different deposition parameters. The starting pressure in the MBE system was typically around $1 \times$

$10^{-10}$ Torr while the pressure during the deposition was around $10^{-8}$ Torr. In the case of sputtering the base pressure was $2 \times 10^{-7}$ Torr and the deposition pressure in Ar atmosphere was around $10^{-3}$ Torr. The different layers were separately deposited by evaporating the single-element targets using 6 kW electron guns in the case of MBE and triode guns in the case of sputtering. The typical deposition rates for Cu and Nb were, respectively, 5.7 and 7.1 Å $s^{-1}$ in the case of sputtering and 0.5–0.6 and 11–13 Å $s^{-1}$ in the case of MBE. In both the systems the deposition rates were controlled by using a quartz crystal oscillating thickness monitor previously calibrated by x-ray reflectivity measurements on deliberately deposited thin films of each material. Moreover, more than one sample (eight in the sputtering and four in the MBE) have been fabricated in the same deposition run in order to obtain the same deposition conditions for all the samples by using specially designed movable shutters. The superconducting properties, transition temperatures $T_C$ and upper critical magnetic fields were resistively measured using a standard dc four-probe technique. The Nb critical temperature was 8.8 K for sputtering prepared samples and 9.2 K in the case of MBE. The crystal structure and the interface quality have been studied by x-ray $\theta$–$2\theta$, polar maps and reflectivity measurements using a Philips X-Pert MRD high resolution diffractometer. Because our research is focused on the effect that the interface between Nb and Cu has on $T$, x-ray reflectivity analysis has been performed on bilayers deliberately realized with appropriate thickness in the same conditions as the trilayers used in superconductivity measurements. These bilayers consist of 100 Å of Nb covering 100 Å of Cu deposited on Si substrate and, alternatively, of 100 Å of Cu upon 100 Å of Nb deposited on Si substrate using both deposition techniques. The thicknesses to be used for this kind of analysis have been decided in advance by means of theoretical simulations of S/N and N/S samples in order to have the best possible reflectivity data.

## 4. Structural characterization

High angle $\theta$–$2\theta$ measurements and polar map acquisition were performed in order to study the in-plane and out-of-plane orientation of the different layers, while low angle reflectivity measurements allowed us to investigate the interface quality and to evaluate the roughness and its correlation length. In all cases, the primary arm of the diffractometer was equipped with a graded parabolic mirror and a 4Ge asymmetric monochromator which allowed us to obtain Cu K$\alpha_1$ radiation ($\lambda = 1.540\,56$ Å) and a divergence of the incident beam of 12 arcsec. For high angle measurements, a beam divergence of 0.5° was obtained by using an appropriate antiscatter slit while a 20-sheet parallel beam collimator with a 0.1 mm slit before the detector was used for low angle measurements. In this last case the divergence of the diffracted beam was 0.1°. The $\theta$–$2\theta$ spectra shown in figures 1(a) and (b) correspond respectively to Cu(1500 Å)/Nb(700 Å)/Cu(1500 Å) obtained by MBE and sputtering, respectively. In both cases, the highest peaks are due to the larger quantity of the correspondent element in the trilayer structure. Nb and Cu have a body centred and face centred cubic structure with a lattice parameter of 3.30 and 3.61 Å respectively [21]. This gives a distance between the (110) and (111) planes of Nb and Cu of 2.33 and 2.08 Å. Our experimental data show that Nb and Cu grow respectively with (110) and (111) planes parallel to the substrate surface as expected. The grains' dimensions in the growth direction, estimated by the Debye–Sherrer formula, are reported in table 1 and they are in agreement with that observed by other authors [15].

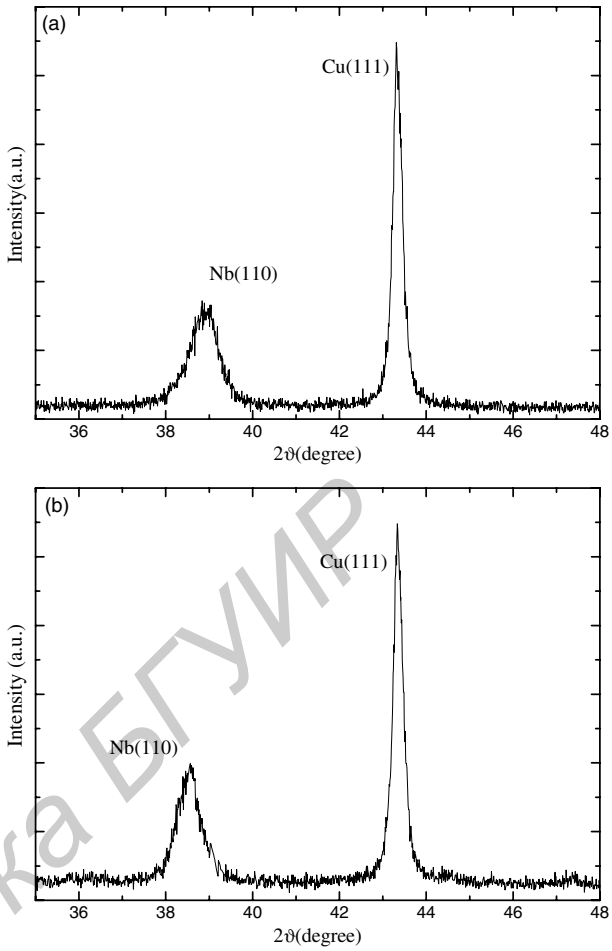


**Figure 1.** $\theta$–$2\theta$ spectra for Cu(1500 Å)/Nb(700 Å)/Cu(1500 Å) trilayer obtained by MBE (a) and sputtering (b).

**Table 1.** Distance between (110) Nb planes, $a_{Nb}$, distance between (111) Cu planes, $a_{Cu}$, Nb and Cu grain dimensions, $D_{Nb}$ and $D_{Cu}$, and lateral roughness correlation length for Nb, $L_{Nb}$, and for Cu, $L_{Cu}$.

| | $a_{Nb}$ (Å) | $a_{Cu}$ (Å) | $D_{Nb}$ (Å) | $D_{Cu}$ (Å) | $L_{Nb}$ (Å) | $L_{Cu}$ (Å) |
|---|---|---|---|---|---|---|
| MBE | 2.310 | 2.090 | 130 | 191 | 300 | 290 |
| Sputtering | 2.310 | 2.086 | 125 | 195 | 210 | 200 |

The distance between the Nb(110) lattice planes is shorter than the expected value. This shrinkage of the distance between the atomic planes is probably due to the strain suffered by this layer when deposited between two Cu layers. This strain could also influence the macroscopic structure as confirmed by the reduced dimension of the (110) Nb grains. Apart from these considerations that concern the growth of the single layers, the deposition technique does not seem to influence the atomic structure in the direction perpendicular to the interfaces.

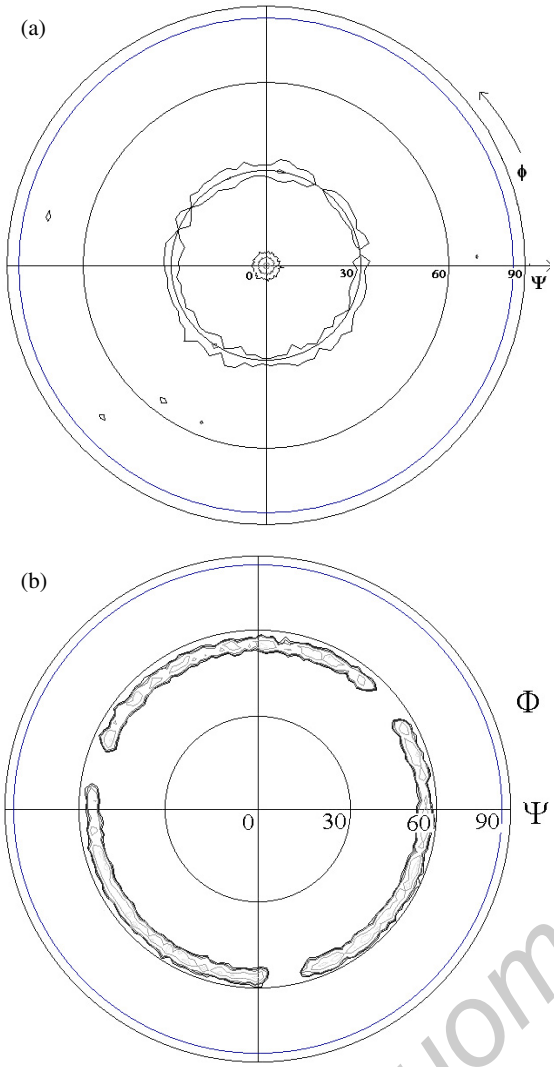


**Figure 2.** Polar maps of Nb(211) (a) and Cu(3$\bar{1}$1) (b) deposited by MBE.

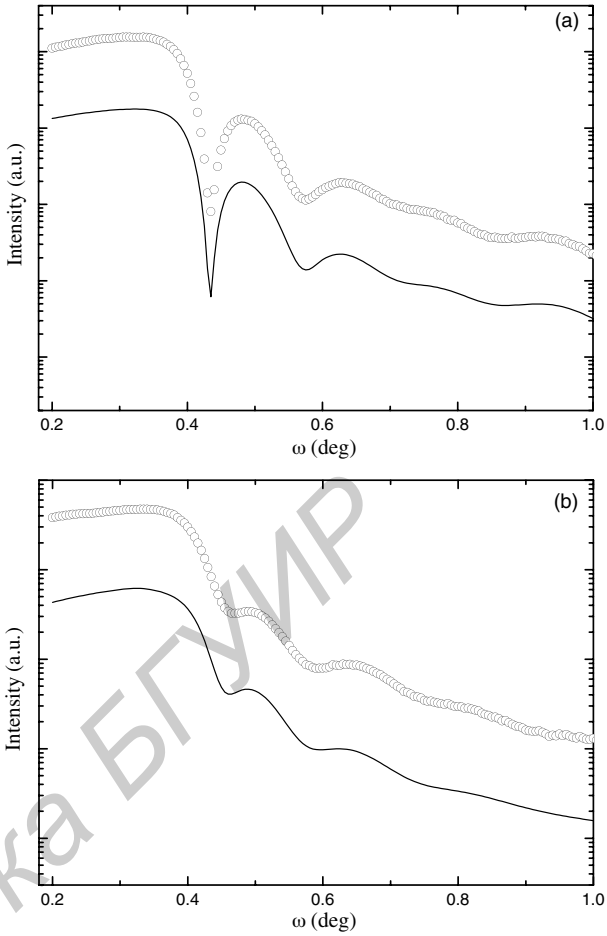


**Figure 3.** Measured (open circles) and simulated (continuous curve) low angle profile for a Cu(100 Å)/Nb(100 Å) bilayer prepared by (a) MBE and (b) sputtering.

In order to study the structure of the different layers along a direction different from the growth, texture measurements were performed on different reflections. In figures 2(a) and (b) polar maps corresponding to the Nb(211) and Cu(3$\bar{1}$1) reflections of the same trilayer deposited by MBE are shown. Similar results were obtained in the case of sputtering. The continuous rings at $\Psi \approx 30°$ and 60° indicate that the in plane axes are not epitaxially oriented and that the different layers grow textured with the (110) and (111) planes parallel to the substrate surface for Nb and Cu respectively. This gives our structures free from in plane mismatch effects because of the lack in any preferred orientation at the interface. Because the same effect is observed both in the case of sputtering and in the case of MBE samples, the absence of in-plane epitaxy is probably due to the fact that the substrates were not heated during the deposition process.

The interface quality were better investigated by reflectivity measurements performed on bilayers Cu/Nb and Nb/Cu appositely deposited by both the systems with 100 Å for each layer. The specular reflectivity profiles are shown in figures 3(a) and (b) for MBE and sputtering respectively together with simulation curves obtained using the Parrat and Nevot–Croce formalism [22, 23] made with the aim to estimate the thickness of the layers and the roughness at the interfaces. The presence of the Kiessing fringes confirm that the layered structure has been achieved. The results of the fits gave a roughness of 18 Å in the case of MBE and 25 Å for sputtering deposited bilayers.

In figure 4 the diffuse spectra (rocking curves) corresponding to the first specular maxima of the reflectivity profile are reported for MBE and sputtering samples respectively. The diffuse spectrum contains information on the vertical and lateral roughness correlation length [24]. To be exact, the presence of satellite peaks indicates a vertical correlation of the roughness whereas the width of the lowest part of the rocking curve is connected to the lateral correlation length of the roughness. The higher the satellite peaks, the stronger the vertical correlation. The experimental data clearly show a stronger vertical correlation of the roughness in the case of MBE with respect to the sputtered samples. Moreover, a rough measure of the lateral correlation length can be obtained by calculating the quantity $L = 2\pi/\Delta q$ where $\Delta q$ is the width in reciprocal lattice units of the lowest part of the diffuse spectrum. This has been done for single Nb and Cu layers and the corresponding results are reported in table 1. Such

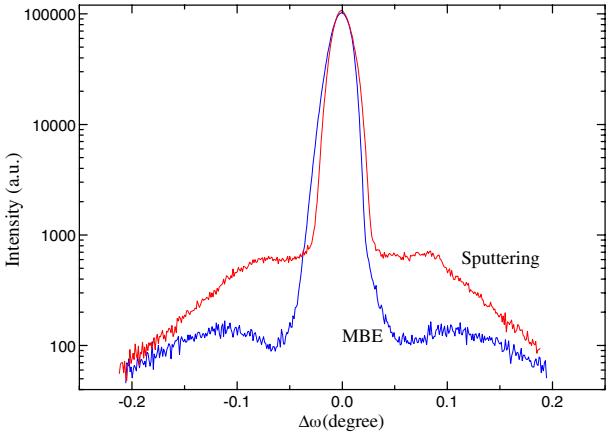


**Figure 4.** Diffuse spectra measured on the first Kiessing fringe of the reflectivity curves for an MBE and a sputtering deposited bilayer.

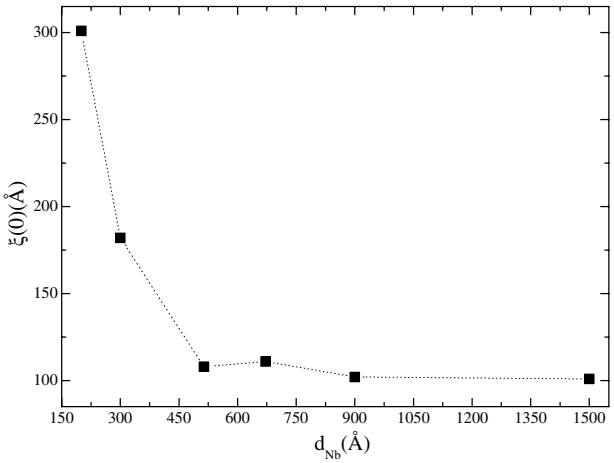


**Figure 5.** Ginzburg–Landau coherence length at zero temperature, $\xi(0)$, versus Nb thickness, $d_{\mathrm{Nb}}$, for Cu/Nb/Cu trilayers prepared by MBE.

values of the roughness and the lateral correlation lengths are observed for other MBE and sputtering deposited samples. These roughness values of the samples obtained by different deposition techniques indicate that the interface fluctuations are negligible with respect to the superconducting correlation length. However, the experimental data also indicate a quite good interface quality of the MBE deposited samples with respect to the sputtered ones.

## 5. Results and discussion

To determine the superconducting coherence length $\xi_S$, we have performed upper critical field measurements of Cu/Nb/Cu trilayers in the direction perpendicular to the sample surface. In this series the external Cu thicknesses were kept constant ($d_{\mathrm{Cu}} = 1500$ Å) while the Nb thickness, $d_{\mathrm{Nb}}$, was varied from 100 to 1500 Å for both the MBE and sputtered series. We have extrapolated the slope $S = \mathrm{d}H_{C2}/\mathrm{d}T|_{T=T_c}$ from the $H_{C2\perp}(T)$ curves by a linear fit near $T_C$ in order to determine the Ginzburg–Landau coherence length at zero temperature $\xi(0)$. In figure 5 we report the behaviour of $\xi(0)$ as a function of $d_{\mathrm{Nb}}$, the Nb thickness present in the sample, obtained from the systematic measurements of $H_{C2\perp}(T)$ performed on Cu/Nb/Cu trilayers prepared by MBE. From this figure it emerges that $\xi(0)$ decreases when increasing $d_{\mathrm{Nb}}$ until a saturation value. In this regime we can think that the observed behaviour for $H_{C2\perp}(T)$ is related to the Nb properties. From this saturation value ($\xi(0) \approx 100$ Å) we have estimated the Nb coherence length, $\xi_{\mathrm{Nb}}$, which is related to $\xi(0)$ by the relation $\xi_{\mathrm{Nb}} = 2\xi(0)/\pi$. In this way a value of $\xi_{\mathrm{Nb}}^{\mathrm{MBE}} = 64$ Å was found in the case of the MBE prepared samples.

To understand how to determine the normal coherence length by the S/N/S trilayers we should consider that, if two S layers are separated by a thin N layer, the decay of the superconducting order parameter from both sides overlaps. By increasing the thickness of the N layer the S layers become more and more decoupled until no overlap is left. For this reason the behaviour of the $T_C(d_N)$ curve will go from a maximum value (related to $T_C$ of the S layer with thickness equal to $2d_S$) to a limiting value (related to the $T_C$ of the single S layer with thickness equal to $d_S$). The

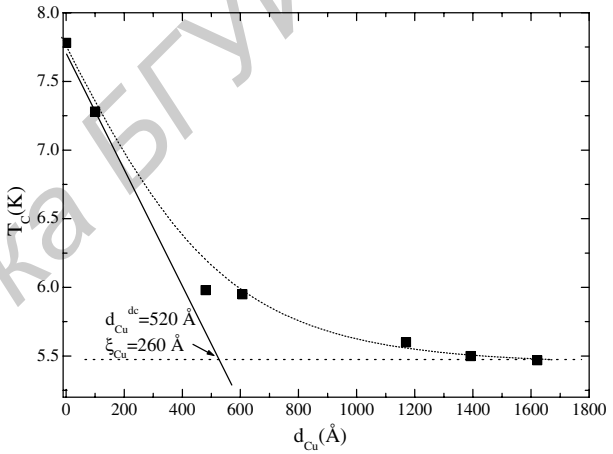


**Figure 6.** Critical temperature, $T_C$, versus Cu thickness, $d_{\mathrm{Cu}}$, for Nb/Cu/Nb trilayers prepared by MBE. The arrow shows the value of $d_{\mathrm{Cu}}^{\mathrm{dc}}$. The solid line indicates the method to determine it. The dashed lines are meant only to guide the eye.

thickness for which the minimum is reached is called the decoupling thickness and corresponds to approximately twice the coherence length ($d_{\mathrm{N}}^{\mathrm{dc}} \approx 2\xi_{\mathrm{N}}$ [3]). Figure 6 shows $T_C$ versus $d_{\mathrm{Cu}}$ measurements performed on Nb/Cu/Nb trilayers ($d_{\mathrm{Nb}} = 220$ Å and $d_{\mathrm{Cu}}$ variable from 0 to 1500 Å). We now identify $d_{\mathrm{Cu}}^{\mathrm{dc}}$ by extrapolation of the steepest slope in the transition curve $T_C(d_{\mathrm{Cu}})$ to the saturation line (dashed line in figure 6) [3]. In this way the value deduced for $\xi_{\mathrm{Cu}}^{\mathrm{MBE}}$ was about 260 Å. Following the same procedure it is possible to determine the Nb and Cu coherence lengths for the samples prepared by sputtering, $\xi_{\mathrm{Nb}}^{\mathrm{Sput}}$ and $\xi_{\mathrm{Cu}}^{\mathrm{Sput}}$.

In table 2 all the measured sample parameters are reported. The obtained values of $\xi_{\mathrm{Nb}}$ and $\xi_{\mathrm{Cu}}$ for both MBE and sputtering are larger than the corresponding roughness value and shorter than the correlation lengths reported in table 1. This indicates that the interface quality does not strongly influence the superconducting properties of our trilayers even though a greater effect is expected in the case of sputtering rather than in MBE deposited samples. Also shown in table 2 are the measured values of the Nb and Cu resistivities, $\rho_{\mathrm{Nb}}$ and $\rho_{\mathrm{Cu}}$, on

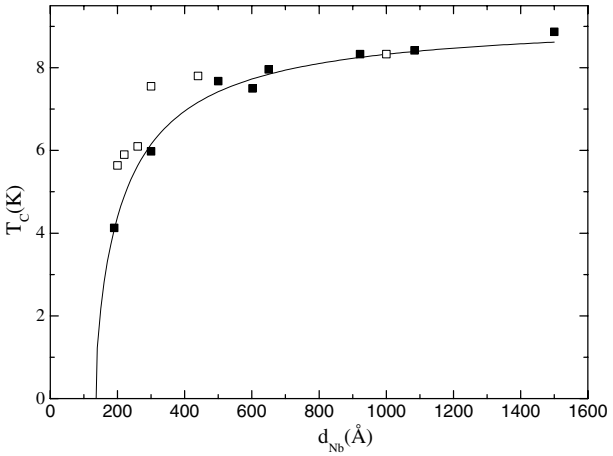


**Figure 7.** Critical temperature, $T_C$, versus $d_{Nb}$ for Cu/Nb/Cu trilayers prepared by MBE. The solid curve is the result of calculation with parameters given in table 2. Open squares refer to single Nb films.

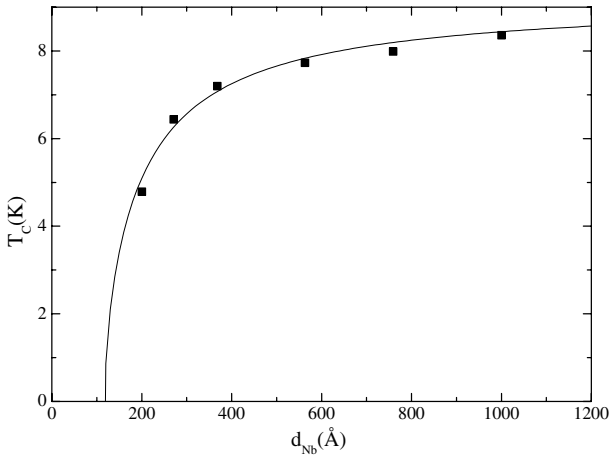


**Figure 8.** Critical temperature $T_C$ versus $d_{Nb}$ for Cu/Nb/Cu trilayers prepared by sputtering. The solid curve is the result of calculation with parameters given in table 2.

**Table 2.** Values of the electrical resistivities, $\rho_{Nb}$ and $\rho_{Cu}$, of the coherence lengths, $\xi_{Nb}$ and $\xi_{Cu}$, for the two materials fabricated with MBE and sputtering techniques. These values have been used in the fit procedure to the Golubov equations to estimate the transparency parameter $\mathcal{T}$.

| | $\rho_{Nb}$ ($\mu\Omega$ cm) | $\rho_{Cu}$ ($\mu\Omega$ cm) | $\xi_{Nb}$ (Å) | $\xi_{Cu}$ (Å) | $\mathcal{T}$ |
|---|---|---|---|---|---|
| MBE | 3.6 | 1.3 | 64 | 260 | $0.30 \pm 0.02$ |
| Sputtering | 4.6 | 1.8 | 67 | 170 | $0.26 \pm 0.02$ |

samples deliberately fabricated both by MBE and sputtering. All these values have been used to reproduce the behaviour of the $T_C(d_{Nb})$ curves for both sets of trilayers and to obtain numerical results for the interface transparency of the two systems (MBE and sputtering).

Figures 7 and 8 show the critical temperature $T_C$ as a function of $d_{Nb}$ for the Cu/Nb/Cu trilayers prepared by MBE and sputtering, respectively (here $d_{Cu} = 1500$ Å and $d_{Nb}$ is variable from 100 to 1500 Å). The transition temperatures of the samples with $d_{Nb} = 100$ Å are not reported because they were below 1.8 K, the lowest reachable temperature with our experimental set-up. In figure 7 are also reported the transition critical temperatures of MBE prepared Nb single films which indicate that the effect of the $T_C(d_{Nb})$ suppression is mainly due to the proximity effect and not to the decreasing Nb thickness. The curve in the figure represents the model calculation according to equations (2) and (3) obtained with only one free parameter, the transparency $\mathcal{T}$. We obtain $\mathcal{T} = 0.30 \pm 0.02$ for MBE prepared samples while $\mathcal{T} = 0.26 \pm 0.02$ for those prepared by sputtering. The obtained value for the interface transparency of Nb/Cu prepared by MBE is therefore only slightly higher than the one obtained in the case of sputtering deposition, for which the reflectivity measurements have shown a higher interface roughness. Moreover the $\mathcal{T}$ values are comparable to others reported in the literature in the case of Nb/Cu layered systems [19, 25]. It is worthy of note that the validity regime of equation (3) is $T_C/T_{CS} \gg \gamma/\gamma_b$. In both our cases we have $\gamma/\gamma_b \approx 0.30$ and $T_C/T_{CS} > 0.5$ in the entire trilayer critical temperature range. Now we can compare these obtained values for $\mathcal{T}$ with the theoretical ones based on the Fermi velocities' mismatch. From equation (1) we get $\mathcal{T} = 0.50$, using $v_{Nb}^F = 2.73 \times 10^7$ cm s$^{-1}$ [26] and $v_{Cu}^F = 1.57 \times 10^8$ cm s$^{-1}$ [21]. However, there are several other factors that have a great influence on the interface transparency which cause a significant reduction of $\mathcal{T}$. For example, the matching between band structures of the two metals plays an important role and this factor influences the transparency even more than Fermi velocities: conduction electrons in Cu have a strong s character while those in Nb have more d-type character and this can lead to a further suppression of $\mathcal{T}$. In addition, in Nb/Cu systems the lattice mismatch, lm, is around 9% ($lm = |l_{Cu} - l_{Nb}|/l_{Nb}$ with $l_{Cu} = 3.61$ Å and $l_{Nb} = 3.30$ Å); this fact, together with the stress caused by the symmetry difference among the fcc-Cu(111) and the bcc-Nb(110) planes, strongly determine the quality of the interface between the two metals. However, from the analysis reported above it seems that the deposition techniques, giving essentially different interface roughness, do not play a strong role in determining the value of $\mathcal{T}$ which seems more related to these intrinsic factors. This result corroborates some recent results obtained on the interface transparency of sputtered Nb/Pd systems which show a higher value for $\mathcal{T}$, essentially due to the very similar values of the Nb and Pd Fermi velocities and band structures [6, 7]. Here we want to mention that the study reported in this paper has also been performed on high quality Nb/Ag trilayers fabricated by MBE. The results we have obtained, using the above reported procedure for Nb/Cu trilayers, have given, for the transparency, $\mathcal{T} = 0.33 \pm 0.02$, very close to that of Nb/Cu. In figure 9 $T_C$ as a function of $d_{Nb}$ for Ag/Nb/Ag trilayers fabricated by MBE is reported. This result agrees with the fact that a very similar theoretical $\mathcal{T}$ value ($\mathcal{T} = 0.55$) can be obtained for Nb/Ag from equation (1) using $v_{Ag}^F = 1.39 \times 10^8$ cm s$^{-1}$ [21].

The effect of the deposition technique on $\mathcal{T}$ has also been studied in external magnetic fields, by measuring the temperature dependence of the parallel upper critical field, $H_{C2\parallel}(T)$. In figure 10 the $H_{C2\parallel}^2(t)$ ($t = T/T_C$ is the reduced critical temperature) dependence is reported for the two Cu/Nb/Cu trilayers having the same layer thickness ($d_{Cu} = 1500$ Å and $d_{Nb} = 200$ Å) but prepared with the two different deposition techniques. The point at which the solid lines no

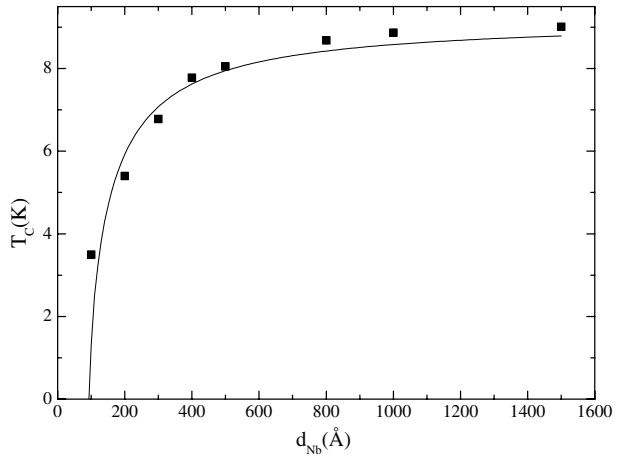


**Figure 9.** Critical temperature, $T_C$, versus $d_{Nb}$ for Ag/Nb/Ag trilayers prepared by MBE. The solid curve is the result of calculation ($\mathcal{T} = 0.33$) with the following measured parameters: $T_{CS} = 9.2$ K, $\rho_{Nb} = 7.3\ \mu\Omega$ cm, $\rho_{Ag} = 4.0\ \mu\Omega$ cm, $\xi_{Nb} = 54$ Å and $\xi_{Ag} = 190$ Å.

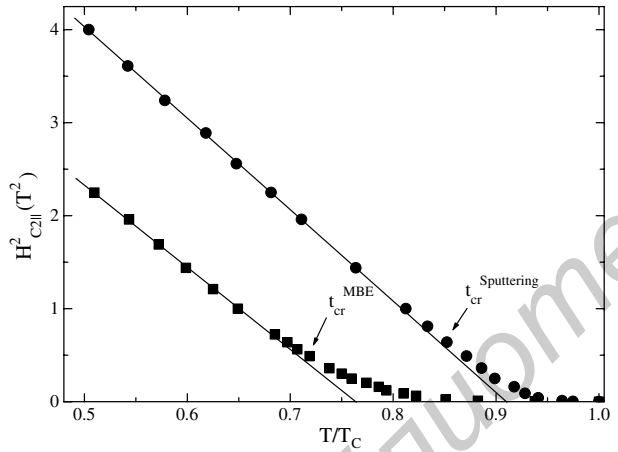


**Figure 10.** Square of the parallel critical magnetic field for Cu/Nb/Cu trilayers prepared by MBE (squares) and sputtering (circles) with $d_{Nb} = 200$ Å versus reduced critical temperature $T/T_C$. The arrows show the dimensional crossover reduced temperature, $t_{CR}$.

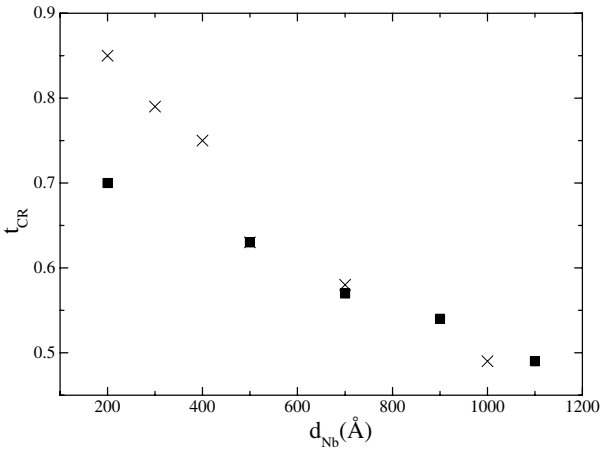


**Figure 11.** Reduced crossover temperature, $t_{CR}$, versus $d_{Nb}$ for Cu/Nb/Cu trilayers prepared by MBE (squares) and sputtering (crosses).

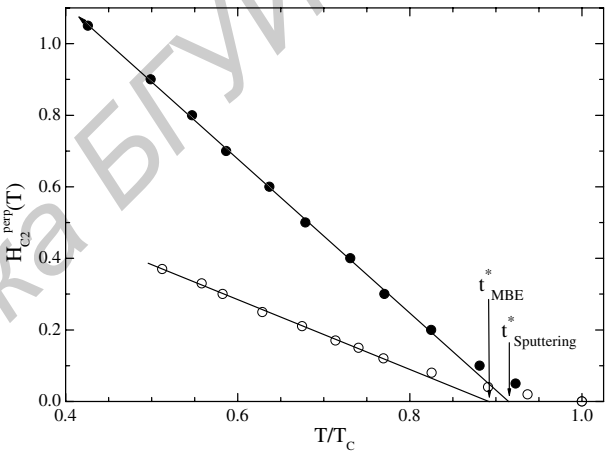


**Figure 12.** Perpendicular critical magnetic field as a function of the reduced temperature $t = T/T_C$ for the Cu/Nb/Cu trilayers with $d_{Cu} = 1500$ Å and $d_{Nb} = 200$ Å obtained by sputtering (closed symbols) and MBE (open symbols). The solid lines are meant to guide the eye.



longer follow the experimental points indicates the 2D–3D reduced crossover temperature $t_{CR}$. We observe that $t_{CR}^{MBE} = 0.70 < t_{CR}^{Sput} = 0.85$ in agreement with what has been recently theoretically predicted [14], confirming that the MBE prepared samples have a higher value of $\mathcal{T}$. These measurements have then been performed on all the other samples of the two series and in figure 11 are reported the $t_{CR}$ for all the samples as a function of the Nb layer thickness. We see that for larger $d_{Nb}$ the $t_{CR}$ values of the MBE and sputtered samples tend to coincide because in this situation the relative effect of the external Cu layer on Nb is weaker. In contrast, for small $d_{Nb}$ values the role played by the interfaces is more relevant and agreement with the predictions is obtained. In this case the effect on the $\mathcal{T}$ value due to the different deposition techniques is more evident (even if only for samples having a thin Nb layer) than observed when analysing the $T_C(d_{Nb})$ curves where the transparency obtained using the Golubov theory is a sort of average value of the interface properties of the entire sample series.

This result is also confirmed when studying the perpendicular upper critical fields, $H_{C2\perp}(T)$, which exhibit a positive curvature close to $T_C$ in both MBE and sputtering fabricated samples. This effect has been recently observed on very similar systems and has been ascribed to the influence of boundary conditions in N/S/N trilayers due to the presence of potential barriers [15]. The effect is pronounced in N/S/N systems and completely absent in an I/S/I configuration as well as for a single Nb film. I here stands for an insulating material. In figure 12 the $H_{C2\perp}(T)$ curves for sputtered and MBE samples having $d_{Nb} = 200$ Å and $d_{Cu} = 1500$ Å are shown. We see that the curvature is more pronounced for the MBE sample with respect to that obtained by sputtering. This observation is consistent with the fact that, due to the smaller value of the interface transparency in sputtered samples, Nb behaves more like an isolated layer. This difference tends to

became smaller and smaller when increasing the Nb thickness in the two sets of trilayers, because the effect of the boundaries tends now to be negligible. Finally, when $d_{Nb} = 1500$ Å the behaviour of $H_{C2\perp}(T)$ in our systems exhibits the usual linear dependence typical of a single Nb film. So again, even though this effect is especially observed in samples having a thin Nb layer, the effect on $\mathcal{T}$ due to the different deposition techniques is quite pronounced and also reflects on the perpendicular critical field behaviour.

## 6. Conclusions

In conclusion, we have studied in the framework of the proximity theory high quality Nb/Cu trilayers realized with two different deposition techniques: sputtering and MBE. The samples have been structurally characterized by extensive x-ray diffraction measurements. The obtained values of the transparency $\mathcal{T}$ (slightly higher for the MBE deposited samples) do not seem strongly influenced by the fabrication methods but more by intrinsic factors such as mismatches of the Fermi velocities and differences between the band and lattice structures of the two metals. The proximity effect in the samples has also been studied in external magnetic fields. In the parallel configuration a significant shift of the 2D–3D crossover temperature has been observed while in the perpendicular case a positive curvature close to the critical temperature has been detected in MBE and sputtered samples. We obtain that the effect of the interface boundaries on the thermodynamic parameters of the trilayers is pronounced for $d_{Nb} < 600$ Å. In this $d_{Nb}$ range both $T_C$ and $H_{C2}$ values are strongly influenced by the $\mathcal{T}$ value. Moreover, the difference in the influence on the $H_{C2}$ values both in parallel and in perpendicular configurations, for samples prepared by different techniques, is very pronounced in spite of the almost equal values of the interface transparency. For this reason the study of the proximity effect in external magnetic fields seems to be a powerful tool to extract information about the boundary resistance of layered systems.

## References


[1] Kupriyanov M Yu and Lukichev V F 1988 *Sov. Phys.—JETP* **67** 1163
[2] Golubov A A 1994 *Proc. SPIE* **2157** 353
[3] Aarts J, Geers J M E, Brück E, Golubov A A and Coehoorn R 1997 *Phys. Rev.* B **56** 2779
[4] Rusanov A, Boogaard R, Hesselberth M, Sellier H and Aarts J 2002 *Physica* C **369** 300
[5] Otop A, Hendrikx R W A, Hesselberth M B S, Ciuhu C, Lodder A and Aarts J 2003 *Preprint* cond-mat/0303393
[6] Cirillo C, Prischepa S L, Salvato M and Attanasio C 2004 *Eur. Phys. J.* B **38** 59
[7] Cirillo C, Prischepa S L, Romano A, Salvato M and Attanasio C 2004 *Physica* C **404** 95
[8] Schöck M, Sürgers C and von Löhneysen H 2000 *Eur. Phys. J.* B **14** 1
[9] de Jong M J M and Beenakker C W J 1995 *Phys. Rev. Lett.* **74** 1657
[10] Vasko V A, Larkin V A, Kraus P A, Nikolaev K R, Grupp D E, Nordman C A and Goldman A M 1997 *Phys. Rev. Lett.* **78** 1134
[11] Dong Z W *et al* 1997 *Appl. Phys. Lett.* **71** 1718
[12] Yeh N C, Vasquez R P, Fu C C, Samoilov A V, Li Y and Vakili K 1999 *Phys. Rev.* B **60** 10522
[13] Sefrioui Z, Arias D, Peña V, Villegas J E, Varela M, Prieto P, León C, Martinez J L and Santamaria J 2003 *Phys. Rev.* B **67** 214511
[14] Ciuhu C and Lodder A 2001 *Phys. Rev.* B **64** 224526
[15] Sidorenko A S, Sürgers C and von Löhneysen H 2002 *Physica* C **370** 197
[16] Schuller I K 1980 *Phys. Rev. Lett.* **44** 1597
[17] Chun C S L, Zheng G-G, Vicent J L and Schuller I K 1984 *Phys. Rev.* B **29** 4915
[18] Koperdraad R T W and Lodder A 1995 *Phys. Rev.* B **14** 9026
[19] Kushnir V N, Prischepa S L, Della Rocca M L, Salvato M and Attanasio C 2003 *Phys. Rev.* B **68** 212505
[20] Usadel K 1970 *Phys. Rev. Lett.* **25** 507
[21] Ashcroft N W and Mermin N D 1976 *Solid State Physics* (Washington, DC: International Thomson Publishing)
[22] Parrat L G 1954 *Phys. Rev.* **95** 359
[23] Nevot L and Croce P 1980 *Rev. Phys. Appl.* **15** 761
[24] Sinha S K, Sirota E B, Garoff S and Stley H B 1988 *Phys. Rev.* B **38** 2297
[25] Geers J M E 1999 *PhD Thesis* Leiden University
[26] Kerchner H R, Christen D K and Sekula S T 1981 *Phys. Rev.* B **24** 1200